

# Person Re-identification in the Wild

Liang Zheng<sup>†\*</sup>, Hengheng Zhang<sup>†\*</sup>, Shaoyan Sun<sup>†\*</sup>, Manmohan Chandraker<sup>§</sup>, Qi Tian<sup>‡</sup>

<sup>†</sup>University of Texas at San Antonio  
of China

<sup>‡</sup>University of Science and Technology  
<sup>§</sup>NEC Labs America

**Abstract.** We present a novel large-scale dataset and comprehensive baselines for end-to-end pedestrian detection and person recognition in raw video frames. Our baselines address three issues: the performance of various combinations of detectors and recognizers, mechanisms for pedestrian detection to help improve overall re-identification accuracy and assessing the effectiveness of different detectors for re-identification. We make three distinct contributions. First, a new dataset, PRW, is introduced to evaluate **Person Re-identification in the Wild**, using videos acquired through six synchronized cameras. It contains 932 identities and 11,816 frames in which pedestrians are annotated with their bounding box positions and identities. Extensive benchmarking results are presented on this dataset. Second, we show that pedestrian detection aids re-identification through two simple yet effective improvements: a discriminatively trained ID-discriminative Embedding (IDE) in the person subspace using convolutional neural network (CNN) features and a Confidence Weighted Similarity (CWS) metric that incorporates detection scores into similarity measurement. Third, we derive insights in evaluating detector performance for the particular scenario of accurate person re-identification.

**Keywords:** Pedestrian detection, person re-identification, convolutional neural networks

## 1 Introduction

Automated entry and retail systems at theme parks, passenger flow monitoring at airports, behavior analysis for automated driving and surveillance are a few applications where detection and recognition of persons across a camera network can provide critical insights. Yet, these two problems have generally been studied in isolation within computer vision. Person re-identification aims to find occurrences of a query person ID in a video sequence, where state-of-the-art datasets and methods start from pre-defined bounding boxes, either hand-drawn [1–3] or automatically detected [4, 5]. On the other hand, several pedestrian detectors achieve remarkable performance on benchmark datasets [6, 7], but little analysis is available on how they can be used for person re-identification.

---

\* Three authors contribute equally to this work.

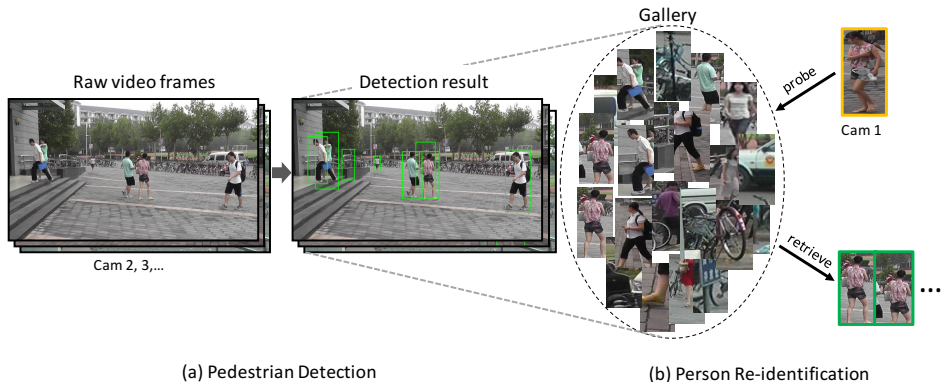


**Fig. 1.** Pipeline of an end-to-end person re-id system. It consists of two modules: pedestrian detection and person recognition (to differentiate from the overall re-id).

In this paper, we propose a dataset and baselines for practical person re-identification in the wild, which moves beyond sequential application of detection and recognition. In particular, we study three aspects of the problem that have not been considered in prior works. First, we analyze the effect of the combination of various detection and recognition methods on person re-identification accuracy. Second, we study whether detection can help improve re-identification accuracy and outline methods to do so. Third, we study choices for detectors that allow for maximal gains in re-identification accuracy.

Current datasets lack annotations for such combined evaluation of person detection and re-identification. Pedestrian detection datasets, such as Caltech [8] or Inria [9], typically do not have ID annotations, especially from multiple cameras. On the other hand, person re-identification datasets, such as VIPeR [10] or Market-1501 [4], usually provide just cropped bounding boxes without the complete video frames, especially at a large scale. As a consequence, a large-scale dataset that evaluates both detection and overall re-identification is needed. To address this, Section 3 presents a novel large-scale dataset called PRW that consists of 932 identities, with bounding boxes across 11,816 frames. The dataset comes with annotations and extensive baselines to evaluate the impacts of detection and recognition methods on person re-identification accuracy.

In Section 4, we leverage the volume of the PRW dataset to train state-of-the-art detectors such as R-CNN [11], with various convolutional neural network (CNN) architectures such as AlexNet [12], VGGNet [13] and ResidualNet [14]. Several well-known descriptors and distance metrics are also considered for person re-identification. However, our joint setup allows two further improvements in Section 4.2. First, we learn an ID-discriminative embedding through classification CNN features, to achieve improved re-id accuracy. Second, we propose a Confidence Weighted Similarity (CWS) metric that incorporates detection scores. Assigning lower weights to false positive detections prevents a drop in re-id accuracy due to the increase in gallery size with the use of detectors.

Given a dataset like PRW that allows simultaneous evaluation of detection and re-identification, it is natural to consider whether any complementarity exists between the two tasks. For a particular re-id method, it is intuitive that a better detector should yield better accuracy. But we argue that the criteria for determining a detector as better are application-dependent. Previous works in pedestrian detection [8, 15, 16] usually use Average Precision or Log-Average Miss Rate under  $\text{IoU} > 0.5$  for evaluation. However, through extensive benchmarking on the proposed PRW dataset, we find in Section 5 that  $\text{IoU} > 0.7$  is a more effective rule in indicating detector influences on re-id accuracy. In other words, the localization ability of detectors plays a critical role in re-id applications.

Figure 1 presents the pipeline of the end-to-end re-id system discussed in this paper. To summarize, our main contributions are:

- A novel large-scale dataset, Person Re-identification in the Wild (PRW), for simultaneous analysis of person detection and re-identification.
- Comprehensive benchmarking of state-of-the-art detection and recognition methods on the PRW dataset.
- Novel insights into how detection aids re-identification, along with an effective descriptor and similarity measure to illustrate how they might be utilized.
- New insights into the evaluation of pedestrian detectors for the specific application of person re-identification.

## 2 Related Work

**An overview of re-id datasets** Several person re-id datasets have been proposed [4, 5, 10, 17, 17, 18]. Varying numbers of IDs and boxes exist with them (see Table 1). These datasets mainly consider variations in lighting, views, scale and so on. Despite some differences among them, a common property is that the pedestrians are confined within pre-defined bounding boxes that are either hand-drawn (for example, VIPeR [10], iLIDS [17], CUHK02 [18]) or obtained using detectors (for example, CUHK03 [5], Market-1501 [4]). But it remains unknown how the quality of detectors affects re-id accuracy. This work makes the initial attempt towards that direction by introducing a dataset that requires considering the entire pipeline for person re-id from scratch.

**Pedestrian detection** Object detection has been successfully moving from the Deformable Part Models (DPM) [6] to CNN-based frameworks such as R-CNN [11] and its variants Fast R-CNN [19] and Faster R-CNN [7]. Recent pedestrian detection works also feature the “proposal+CNN” approach. Pedestrian detection usually employs weak pedestrian detectors as proposals, which allows achieving relatively high recall using very few proposals. For example, DBN-Isol [20] and DBN-Mut [21] both use DPM as proposals, while JointDeep [16] and SDN [22] use the HOG+CSS+linear SVM detector as proposals. Despite the impressive recent progress in pedestrian detection, it has been rarely considered with person re-identification as an application. This paper attempts to determine how detection can help re-id and provide insights in assessing detector performance.

**Person re-identification** Recent progress in person re-identification mainly consists of advances in features and metrics. Examples of hand-crafted features include color and texture histograms [4, 23], symmetry-driven accumulation of local features [24] and so on. For measuring feature similarities, previous works focus on designing distance metrics [1, 25, 26]. For example, Cross-view Quadratic Discriminant Analysis (XQDA) [1] simultaneously learns a low-dimensional subspace and a discriminative metric. Several recent works [5, 27–29] focus on learning features and metrics through the CNN framework. Formulating person re-id as a ranking task, image pairs [5, 27, 29] or triplets [28] are fed into the CNN instead of single training images as in the classification or detection cases. In this work, with a sufficient amount of training data per identity, we propose to learn an ID-discriminative embedding in the pedestrian subspace through classic CNN frameworks. This method proves effective in our experiments.

**Detection and re-identification** In our knowledge, two previous works focus on such end-to-end systems. In [30], persons in photo albums are detected using poselets [31] and recognition is performed using face and global signatures. However, the setting in [30] is not typical for person re-identification where pedestrians are observed by surveillance cameras and faces are not clear enough. In a work closer to ours, Xu *et al.* [32] propose to jointly model pedestrian commonness and uniqueness, and calculate the similarity between query and each sliding window in a brute-force manner. While [32] works on datasets consisting of no more than 214 video frames, it would have efficiency issues with practical large-scale datasets. Departing from both works, this paper sets up a large-scale benchmark system to jointly analyze detection and re-id performance in depth.

## 3 The PRW Dataset

### 3.1 Annotation Description

The PRW dataset is an extension of the Market-1501 dataset [4]. We acquire the original video frames as well as the box annotations from the authors of [4] and significantly extend them. The videos are collected on a university campus and are of total length 10 hours. This aims to mimic the application in which a person-of-interest goes out of the field-of-view of the current camera for a short duration and needs to be located from nearby cameras. A total of 6 cameras were used, among which 5 are 1080×1920 HD and 1 is 576×720 SD. The video captured by each camera is annotated every 25 frames (1 second in duration). We first manually draw a bounding box for all pedestrians who appear in the frames and then assign an ID if it exists in the Market-1501 dataset. Since all pedestrians are boxed, when we are not sure about a person’s ID (ambiguity), we assign  $-2$  to it. These ambiguous boxes are used in detector training and testing, but are excluded in re-identification training and testing. Figure 2 and Figure 3 show the annotation interface and sample detected boxes, respectively.

A total of 11,816 frames are manually annotated to obtain 43,110 pedestrian bounding boxes, among which 34,304 pedestrians are annotated with an ID

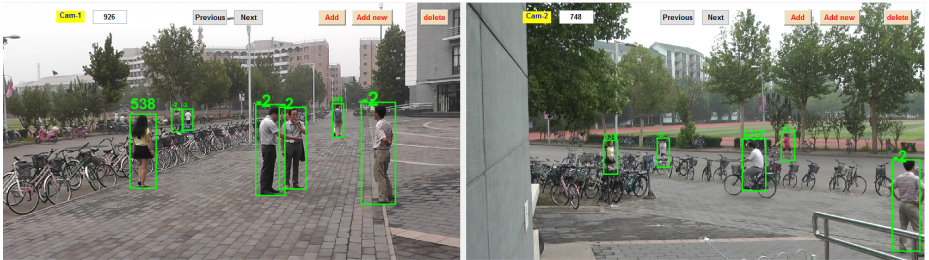


**Fig. 2.** Annotation interface. All appearing pedestrians are annotated with a bounding box and ID. ID ranges from 1 to 932, and -2 stands for ambiguous persons

Datasets	#frame	#ID	#anno. box	#box/ID	#gallery box	#cam.
<b>PRW</b>	11,816	932	34,304	36.8	100-500k	6
CAMPUS [33]	214	74	1,519	20.5	1519	3
EPFL [34]	80	30	294	9.8	294	4
Market-1501 [4]	0	1,501	25,259	19.9	19,732	6
RAiD [35]	0	43	6,920	160.9	6,920	4
VIPeR [10]	0	632	1,264	2	1,264	2
i-LIDS [17]	0	119	476	2	476	2
CUHK03 [5]	0	1,360	13,164	9.7	13,164	2

**Table 1.** Comparing PRW with existing datasets [4, 5, 10, 17, 35, 36]

ranging from 1 to 932 and the rest are assigned an ID of  $-2$ . In Table 1, we compare the new dataset with previous person re-id datasets in terms of numbers of frames, IDs, annotated boxes, annotated boxes per ID, gallery boxes and number of cameras. Specifically, since we densely label all the subjects, the number of boxes for each identity is almost twice that of Market-1501. Moreover, when forming the gallery, the detectors produce 100k-500k boxes depending on the threshold. The distinctive feature enabled by the PRW dataset is the end-to-end evaluation of person re-identification systems. This dataset provides the original video frames along with hand-drawn ground truth bounding boxes, which makes it feasible to evaluate both pedestrian detection and person re-identification. But more importantly, PRW enables assessing the influence of pedestrian detection on person re-identification, which is a topic of great interest for practical applications but rarely considered in previous literature.

### 3.2 Evaluation Protocols

The PRW dataset is divided into a training set with 5,704 frames and 482 IDs and a test set with 6,112 frames and 450 IDs. We choose this split since it enables the minimum ID overlap between training and testing sets. Detailed statistics of the splits are presented in Table 2.

**Pedestrian Detection** A number of popular pedestrian datasets exist, to name a few, INRIA [9], Caltech [8] and KITTI [37]. The INRIA dataset contains 1,805



**Fig. 3.** Examples of detected bounding boxes from video frames in the PRW dataset. In “persons w/ID”, each column contains 4 detected boxes of the same identity from distinctive views. Column “persons w/o ID” presents persons who do not have an ID in the dataset. Column “background” shows false positive detection results. The detector used in this figure is DPM + RCNN (AlexNet).

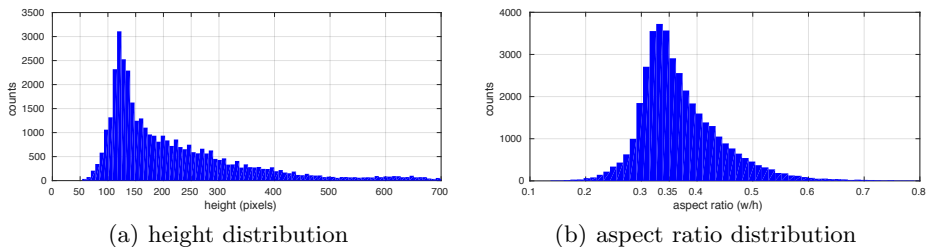


**Fig. 4.** Distribution of pedestrian heights and aspect ratio in PRW.

128×64 pedestrian images cropped from personal photos; the Caltech dataset provides ~350k bounding boxes from ~132k frames; the KITTI dataset has 80k labels for the pedestrian class. With respect to the number of annotations, PRW (~43k boxes) is a medium-sized dataset for pedestrian detection. The training and testing splits are as described above and in Table 2. Following the protocols in KITTI as well as generic object detection, we mainly use the precision-recall curve and average precision to evaluate detection performance. We also report the log-average miss rate (MR) proposed in [8]. More statistics about the annotated pedestrians can be viewed in Fig. 4.

**Person Re-identification** A good re-id system possesses two characteristics. First, all pedestrians are accurately localized within each frame, that is, 100% recall and precision. Second, given a probe pedestrian, all instances of the same person captured by disjoint cameras are retrieved among the top-ranked results.

Datasets	# frames	# ID	# ped.	# ped. w/ ID	# ped. w/o ID
Train	5,134	482	16,243	13,416	2,827
Validation	570	482	1,805	1,491	314
Test	6,112	450	25,062	19,127	5,935

**Table 2.** Training/validation/testing splits of the PRW dataset

Re-identification is a 1:N search process. On the one hand, queries are produced by hand-drawn bounding boxes, as in practice, it takes acceptable time and effort for a user to draw a bounding box on the person-of-interest. For each ID, we randomly select one query under each camera. In total, we have 2,057 query images for the 450 IDs in the test set, averaging 4.57 (maximum 6) queries/ID. On the other hand, “N” denotes the database or gallery. A major difference between PRW and traditional re-id datasets [4, 5, 10, 17, 35, 36] is that the gallery in PRW varies with the settings of pedestrian detectors. Different detectors will produce galleries with different properties; even for the same type of detector, varying the detection threshold will yield galleries of different sizes. A good detector will be more likely to recall the person-of-interest while keeping the database small.

The IDs of the gallery boxes are determined by their intersection-over-union (IoU) scores with the ground truth boxes. In accordance to the practice in object detection, the detected boxes with IoU scores larger than 0.5 are assigned with an ID, while those with IoU less than 0.5 are determined as distractors [4]. Now, assume that we are given a query image  $I$  and a gallery  $\mathcal{G}$  generated by a specific detector. We calculate the similarity score between the query and all gallery boxes to obtain a ranking result. Following [4], two metrics are used to evaluate person re-id accuracy – mean Average Precision (mAP), which is the mean across all queries’ Average Precision (AP) and the rank-1, 10, 20 accuracy denoting the possibility to locate at least one true positive in the top-1, 10, 20 ranks.

Combining pedestrian detection, we plot mAP (or rank-1, rank-20 accuracy) against the average number of detected boxes per image to present the end-to-end re-id performance. Conceptually, with few detection boxes per image, the detections are accurate but recall is low, so a small mAP is expected. When more boxes are detected, the gallery is filled with an increasing number of false positive detections, so mAP will first increase due to higher recall and then drop due to the influence of distractors.

## 4 Base Components and Proposed Improvements

### 4.1 Base Components in the End-to-End System

**Pedestrian detection** Recent state-of-the-art in pedestrian detection usually adopts the “proposal+CNN” approach [38, 39]. Instead of using objectness proposals such as selective search [40], hand-crafted pedestrian detectors are first applied to generate proposals. Since these weak detectors are discriminatively trained on pedestrians, it is possible to achieve good recall with very few proposals (in the order of 10). While RCNN is slow with 2000 proposals, extracting CNN

features from a small number of proposals is fast, so we use RCNN instead of the fast variant [19]. Specifically, the feature for detection can be learnt through the RCNN framework by classifying each box into 2 classes, namely pedestrian and background. In this paper, three CNN architectures are tested – AlexNet [12], VGGNet [13] and ResidualNet [14].

**Person re-identification** The person re-id component has two modules: image descriptor and distance metric. For image descriptor, we test 6 state-of-the-art methods, namely BoW [4], LOMO [1], gBiCov [2], HistLBP [3], SDALF [24] and the IDE recognizer we propose in Section 4.2. For metric learning algorithms, the 4 tested methods are KISSME [26], XQDA [1], DVR [41] and the Discriminative Null Space (DNS) [25]. Given a probe image  $\mathbf{x} \in \mathcal{R}^d$  in a  $d$ -dim space and a gallery image  $\mathbf{y} \in \mathcal{R}^d$ , the distance function between  $\mathbf{x}$  and  $\mathbf{y}$  can be written as  $d(\mathbf{x}, \mathbf{y}) = (\mathbf{x} - \mathbf{y})^\top \mathcal{M}(\mathbf{x} - \mathbf{y})$ , where  $\mathcal{M}$  is a matrix learned in the training data. It reduces to Euclidean distance if  $\mathcal{M}$  is the identity matrix. For KISSME,  $\mathcal{M}$  is composed of the covariance matrices of the inter-class and intra-class variations. For XQDA,  $\mathcal{M}$  further contains a kernel matrix for subspace learning.

## 4.2 Proposed Improvements

**ID-discriminative Embedding** Prior state-of-the-art methods using deep networks for person re-id typically employ Siamese models. This is primarily attributable to the fact that current datasets have a small number of boxes per ID and there is simply not enough data to train a network like the AlexNet. In this work, with the PRW dataset, we are able to train standard CNN-based classification models using the training boxes per ID (class). Specifically, the training samples per ID consist of both hand-drawn and detected boxes. In PRW, the average number of training samples per ID is over 50. During the training process, an embedding in the person subspace is learned to discriminate different identities. Then during testing, features of the detected bounding box are extracted from the fully connected layer (or the pool5 layer in ResidualNet), following which Euclidean distance or other learned metrics are used to calculate the similarity between probe and gallery images.

**Confidence Weighted Similarity** Previous works treat all gallery boxes as equal in estimating their similarity with the query. This results in a problem: when populated with false detections on the background (inevitable when gallery gets larger with the use of detectors), re-id accuracy will drop with the gallery size [4]. This work proposes to address this problem by incorporating detection confidence into the similarity measurement. Intuitively, false positive detections will receive lower weights and will have reduced impact on re-id accuracy. Specifically, detector confidences of all gallery boxes are linearly normalized to  $[0, 1]$  in a global manner. Then, the cosine distance between two descriptors are calculated, before multiplying the normalized confidence. Currently, this method supports cosine (Euclidean) distance between descriptors, but in future works, more sophisticated weightings corresponding to metric learning methods may also be considered.

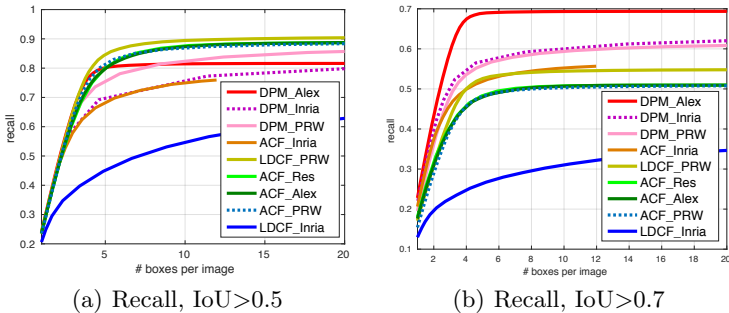


**Fig. 5.** Detection recall at two IoU criteria. “Inria” and “PRW” denote models trained on INRIA [9] and the proposed PRW datasets, respectively. “Alex” and “Res” denote RCNN models fine tuned with AlexNet [12] and ResidualNet [14], respectively.

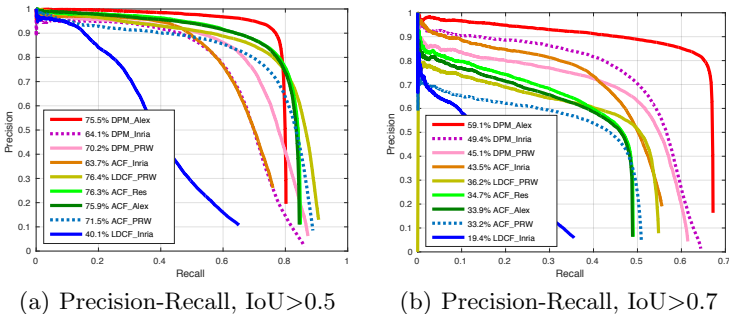


**Fig. 6.** Precision-recall curves at two IoU criteria. Detectors are the same as Fig. 5. The Average Precision number is shown before the name of each method.

## 5 Experiments

### 5.1 Evaluation of Pedestrian Detection

First, we evaluate the detection recall of several important detection models on PRW. This serves as an important reference to the effectiveness of proposals for RCNN based methods. These models include Deformable Part Model (DPM) [6], Aggregated Channel Features (ACF) [42] and Locally Decorrelated Channel Features (LDCF) [43]. We also test their respective RCNN versions. We retrain these models on the PRW training set and plot detection recall against average number of detection boxes per image on the testing set. The results are shown in Fig. 5. It is observed that recall for the best detectors reaches around 90% for  $\text{IoU} > 0.5$ , and around 60% for  $\text{IoU} > 0.7$ .

The detection methods without RCNN mentioned above are used as proposals, and are subsequently coupled with RCNN based models. Specifically, we fine tune RCNN with three CNN models – AlexNet (Alex) [12], VGGNet (VGG) [13], and ResidualNet (Res) [14]. Additionally, we report results of the Histogram of

Methods	IoU > 0.5		IoU > 0.7		Time (sec)
	AP (%)	MR (%)	AP (%)	MR (%)	
DPM_Alex	75.5	<b>39.9</b>	<b>59.1</b>	<b>63.6</b>	6.7
DPM_Inria	64.1	64.7	49.4	76.0	6.5
DPM	70.2	61.5	45.1	81.9	6.5
ACF_Inria	63.7	61.5	43.5	79.9	2.7
LDCF	76.4	58.4	36.2	87.2	1.4
ACF_RES	76.3	50.8	34.1	84.2	2.7
ACF_Alex	75.9	50.9	33.9	85.4	2.7
ACF	71.5	65.1	33.2	89.6	2.7
ACF_VGG	<b>76.8</b>	50.2	33.3	85.2	2.7
LDCF_Inria	40.1	80.3	19.4	92.9	1.4
CCF_Caltech	59.6	72.7	10.6	98.7	8.8
HOG_Inria	11.2	97.2	1.0	99.8	1.9

**Table 3.** Performance of various detectors trained and tested on the proposed PRW dataset. Average Precision (AP) and Miss Rate (MR) are reported. Whenever RCNN is trained, we use bounding box regression and non-maximum suppression as well.

Oriented Gradient (HOG) [9] as well as the recently proposed Convolutional Channel Features (CCF) [44]. True positives are defined by  $\text{IoU} > 0.5$  or  $\text{IoU} > 0.7$ . We report both the Average Precision (AP) and Log Average Miss Rate (MR). Experimental results are presented in Fig. 6 and Table 3. As IoU increases, detector performance deteriorates significantly which is observed in [8]. Under  $\text{IoU} > 0.7$ , the best detector is DPM+AlexNet, having an AP of 59.1%, which is +9.7% higher than the second best detector. The reason that DPM has robust performance under larger IoU is that it consists of multiple components (parts) which adapts well to pedestrian deformation, while channel feature based methods typically set aspect ratio types that are less robust to target variations. In both detection recall and detection accuracy experiments, we find that detector rankings are different from  $\text{IoU} > 0.5$  to  $\text{IoU} > 0.7$ . With respect to detection time, it takes 2.7s, 1.4s, and 6.5s on average on a  $1080 \times 1920$  frame for ACF, LDCF and DPM, respectively, using MATLAB 2015B on a machine with 16GB memory, K40 GPU and Intel i7-4770 Processor. RCNN requires 0.2s for 20 proposals.

## 5.2 Evaluation of Person Re-identification

We benchmark the performance of some recent descriptors and metrics on the PRW dataset. Various types of detectors are used – DPM, ACF, LDCF and their related RCNN methods. The results are shown in Fig. 7 and Table 4. We observe that for hand-crafted features, “HistLBP+DNS” outperforms others when built on the DPM-AlexNet detector. These results generally agree with observations in prior works [25]. We conjecture that given a fixed detector, re-identification accuracy will display similar trends as prior studies [3, 5, 25].

Detector	Recognizer	#detection=3			#detection=5			#detection=10		
		mAP	r1	r20	mAP	r1	r20	mAP	r1	r20
DPM	BOW	8.9	30.4	58.3	9.7	31.1	58.6	9.6	30.5	57.7
DPM	IDE	12.7	37.2	72.2	13.7	36.9	72.1	13.7	36.6	70.8
DPM	IDE <sub>det</sub>	17.2	45.9	77.9	18.8	45.9	77.4	19.2	45.7	76.0
DPM-Alex	SDALF+Kiss.	12.0	32.6	63.8	13.0	32.5	63.4	12.4	31.8	
DPM-Alex	LOMO+XQ.	13.4	34.9	66.5	13.0	34.1	64.0	12.4	33.6	62.5
DPM-Alex	HistLBP+DNS	14.1	36.8	70.0	13.6	35.9	67.8	12.7	35.0	65.7
DPM-Alex	IDE	15.1	38.8	74.1	14.8	37.6	71.4	14.1	36.9	69.8
DPM-Alex	IDE <sub>det</sub>	<b>20.2</b>	<b>48.2</b>	78.1	20.3	47.4	77.1	19.9	47.2	76.4
DPM-Alex	IDE <sub>det</sub> +CWS	<b>20.0</b>	<b>48.2</b>	<b>78.8</b>	<b>20.5</b>	<b>48.3</b>	<b>78.8</b>	<b>20.5</b>	<b>48.3</b>	<b>78.8</b>
ACF	LOMO+XQ.	10.5	31.5	61.6	10.5	30.9	59.5	9.7	29.7	57.4
ACF	gBiCov+Kiss.	9.8	31.1	60.1	9.9	30.3	58.3	9.0	29.0	55.9
ACF	IDE <sub>det</sub>	16.6	44.8	75.9	17.5	43.8	76.0	17.0	42.9	74.5
ACF-Res	IDE	12.4	35.0	70.4	12.5	33.8	68.6	11.5	33.0	66.7
ACF-Alex	LOMO+XQ.	10.5	31.8	60.7	10.3	30.6	59.4	9.5	29.6	57.1
ACF-Alex	IDE <sub>det</sub>	17.0	45.2	76.6	17.5	43.6	75.1	16.6	42.7	73.7
ACF-Alex	IDE <sub>det</sub> +CWS	17.0	45.2	76.8	17.8	45.2	76.8	17.8	45.2	76.8
LDCF	BoW	8.2	30.1	56.9	9.1	29.8	57.0	8.3	28.3	55.3
LDCF	LOMO+XQ.	11.2	31.6	62.9	11.0	31.1	62.2	10.1	29.6	58.6
LDCF	gBiCov+Kiss.	9.5	30.7	58.8	9.6	30.1	58.4	8.8	28.7	56.7
LDCF	IDE	12.7	35.3	70.1	34.4	13.1	69.4	12.2	33.1	68.0
LDCF	IDE <sub>det</sub>	17.5	45.3	76.2	18.3	44.6	75.6	17.7	43.8	74.3
LDCF	IDE <sub>det</sub> +CWS	17.5	45.5	76.3	18.3	45.5	76.4	18.3	45.5	76.4

**Table 4.** Results of various combinations of detectors and recognizers on PRW dataset.

### 5.3 Impact of detectors on re-identification

**Criteria for detector assessment** To find how re-id accuracy varies with detector performance, we systematically test 9 detectors (as described in Fig. 5 and Fig. 6) and 3 recognizers. The 3 recognizers are: 1) 5,600-dimensional Bag-of-Words (BoW) descriptor [4], the state-of-the-art unsupervised descriptor, 2) 4,096-dimensional CNN embedding feature described in Section 4.2 using AlexNet, and 3) LOMO+XQDA [1], a state-of-the-art supervised recognizer. From the results in Fig. 7 and Table 4, a key finding is that *given a recognizer, the re-id performance is consistent with detector performance evaluated using the IoU > 0.7 criterion*. In fact, if we use the IoU > 0.5 criterion as most commonly employed in pedestrian detection, our study shows that the detector rankings do not have accurate predictions on re-id accuracy. Specifically, while the ‘‘DPM-Alex’’ detector ranks 4th in average precision (75.5%) with the IoU > 0.5 rule, it enables superior re-id performance which is suggested in its top ranking under IoU > 0.7. The same observations hold for the other 8 detectors. This conclusion can be attributed to the explanation that under normal circumstances, a better localization result will enable more accurate matching between the query and gallery boxes. As an insight from this observation, when a pool of detectors is available in a practical person re-identification system, a good way for choosing the optimal one is to rank the detectors according to their performance under

IoU > 0.7. In addition, recent research on partial person re-identification [45] may be a possible solution to the problem of misalignment.

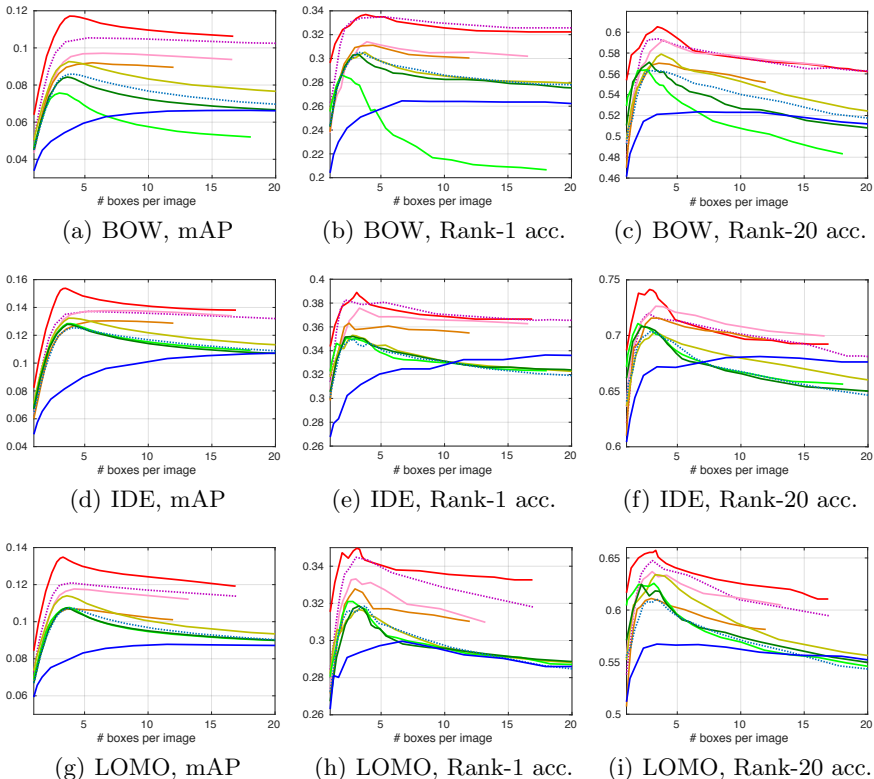


**Fig. 7.** Re-id accuracy (mAP, rank-1 accuracy, and rank-20 accuracy) with 9 detectors and 3 recognizers. Legends are the same as Fig. 5 and Fig. 6.

**Effectiveness of ID-discriminative Embedding** We discuss two variants of IDE. For the first variant, we fine tune IDE directly from AlexNet pre-trained on ImageNet, denoted as  $IDE_{imgnet}$ . For the second variant, we first fine tune a pedestrian detection model (2 classes, pedestrian and background) from AlexNet pre-trained on ImageNet, and then we further fine tune it using the IDE method described in Section 4.2. We denote the second variant as  $IDE_{det}$ . Experimental results related to the IDE variants are presented in Table 4 and Fig. 8.

Two major conclusions can be drawn from the above experiments. First, we observe that the accuracy of IDE is superior to that of hand-crafted descriptors, and is further improved in combination with state-of-the-art metric learning schemes. Second, it is noticeable that  $IDE_{det}$  yields considerably higher re-id accuracy than  $IDE_{imgnet}$ . Specifically, when using the DPM detector trained

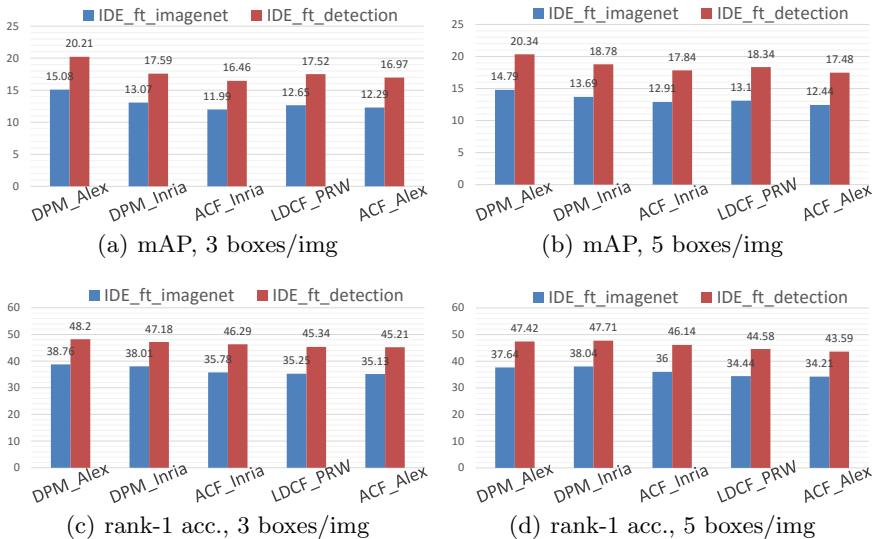


**Fig. 8.** Plots of mAP and rank-1 accuracy using two variants of the proposed IDE with 5 detectors. Fine tuning on the pedestrian-background detection model improves over fine tuning on the Imagenet model.

on INRIA dataset and considering 3 detection boxes per image,  $IDE_{det}$  results in +4.52% and +9.17% improvement in mAP and rank-1 accuracy, respectively. Very similar improvements can be observed for the other 4 detectors and using 5 detection boxes per image. This indicates that when more background and pedestrian samples are “seen”, the re-id feature is more robust against outliers. In fact, a promising direction is to utilize more background and pedestrian samples without ID that are cheaper to collect in order to pre-train the IDE model.

**Effectiveness of Confidence Weighted Similarity (CWS)** We test the CWS proposed in Section 4.2 on the PRW dataset with three detectors and the  $IDE_{det}$  descriptor. The results are shown in Fig. 9. The key observation is that CWS is extremely effective in preventing re-id accuracy from dropping as the number of detections per image increase. As discussed before, more distractors are present when the database get larger and CWS addresses the problem by suppressing the scores of false positive results. In Table 4, the best results on the PRW dataset are achieved when CWS is used, which illustrates the effectiveness of the proposed similarity. We will extend CWS to include metric learning representations in the future work. Figure 10 presents some sample re-id results.

## 6 Conclusions and Future Work

We have presented a novel large-scale dataset, baselines and metrics for end-to-end person re-identification in the wild. The proposed PRW dataset has a

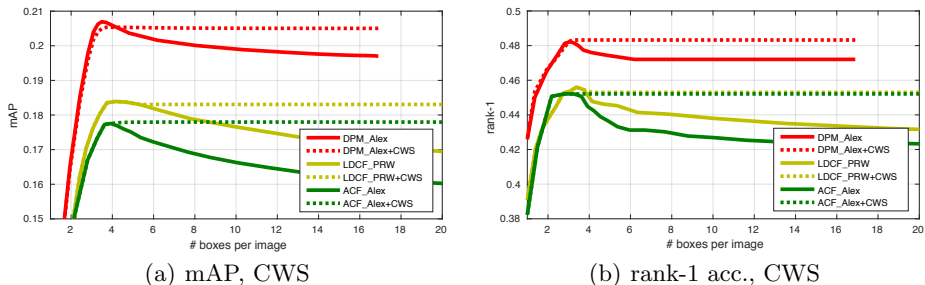


**Fig. 9.** Effectiveness of the proposed Confidence Weighted Similarity (CWS) on the PRW dataset. We test three detectors and the IDE descriptor fine-tuned on the pedestrian-background detection model.

number of features that are not present in previous re-id datasets, allowing the first systematic study of how the interplay of pedestrian detection and person re-identification affects the overall performance. Besides benchmarking several state-of-the-art methods in the fields of pedestrian detection and person re-identification, this paper also proposes two effective methods to improve the re-id accuracy, namely, ID-discriminative Embedding and Confidence Weighted Similarity. Further, our extensive experiments serve as a guide to selecting the best detectors and detection criteria for the specific application of person re-identification.

Our work also enables multiple directions for future research. First, it is critical to design effective bounding box regression schemes to improve person matching accuracy. Apart from hand-drawn queries, one can also generate multiple queries to mimic detection misalignment. Second, given the baseline method proposed in this paper to incorporate detection confidence into similarity scores, more sophisticated re-weighting schemes based on metric learning can be devised. This direction could not have been enabled without a dataset that jointly considers detection and re-identification. Third, while it is expensive to manually assign IDs, annotation of pedestrian boxes without IDs is relatively easier and large amounts of pedestrian data already exist. According to the IDE results reported in this paper, it will be of great value to utilize such weakly-labeled data to improve re-id performance. Finally, effective partial re-id algorithms [45] can be important for end-to-end systems on the PRW dataset (Fig. 10).



**Fig. 10.** Sample re-identification results on the proposed PRW dataset with the DPM\_Alex detector and the proposed IDE descriptor. Rows 1 and 2 are success cases, while Rows 3 and 4 are failure cases due to similar clothing and truncation, respectively. With truncated queries, partial re-id methods [45] might be especially important.

## References

1. Liao, S., Hu, Y., Zhu, X., Li, S.Z.: Person re-identification by local maximal occurrence representation and metric learning. In: CVPR. (2015)
2. Ma, B., Su, Y., Jurie, F.: Covariance descriptor based on bio-inspired features for person re-identification and face verification. *Image and Vision Computing* **32**(6) (2014) 379–390
3. Xiong, F., Gou, M., Camps, O., Sznaiar, M.: Person re-identification using kernel-based metric learning methods. In: ECCV. (2014) 1–16
4. Zheng, L., Shen, L., Tian, L., Wang, S., Wang, J., Tian, Q.: Scalable person re-identification: A benchmark. In: ICCV. (2015)
5. Li, W., Zhao, R., Xiao, T., Wang, X.: Deepreid: Deep filter pairing neural network for person re-identification. In: CVPR. (2014) 152–159
6. Felzenszwalb, P.F., Girshick, R.B., McAllester, D., Ramanan, D.: Object detection with discriminatively trained part-based models. *Pattern Analysis and Machine Intelligence, IEEE Transactions on* **32**(9) (2010) 1627–1645
7. Ren, S., He, K., Girshick, R., Sun, J.: Faster r-cnn: Towards real-time object detection with region proposal networks. In: *Advances in Neural Information Processing Systems*. (2015) 91–99
8. Dollar, P., Wojek, C., Schiele, B., Perona, P.: Pedestrian detection: An evaluation of the state of the art. *Pattern Analysis and Machine Intelligence, IEEE Transactions on* **34**(4) (2012) 743–761
9. Dalal, N., Triggs, B.: Histograms of oriented gradients for human detection. In: *Computer Vision and Pattern Recognition, 2005. CVPR 2005. IEEE Computer Society Conference on*. Volume 1., IEEE (2005) 886–893
10. Gray, D., Brennan, S., Tao, H.: Evaluating appearance models for recognition, reacquisition, and tracking. In: *Proc. IEEE International Workshop on Performance Evaluation for Tracking and Surveillance*. (2007)
11. Girshick, R., Donahue, J., Darrell, T., Malik, J.: Rich feature hierarchies for accurate object detection and semantic segmentation. In: CVPR. (2014)
12. Krizhevsky, A., Sutskever, I., Hinton, G.E.: Imagenet classification with deep convolutional neural networks. In: NIPS. (2012)
13. Simonyan, K., Zisserman, A.: Very deep convolutional networks for large-scale image recognition. arXiv preprint arXiv:1409.1556 (2014)
14. He, K., Zhang, X., Ren, S., Sun, J.: Deep residual learning for image recognition. arXiv preprint arXiv:1512.03385 (2015)
15. Zhang, S., Benenson, R., Omran, M., Hosang, J., Schiele, B.: How far are we from solving pedestrian detection? arXiv preprint arXiv:1602.01237 (2016)
16. Ouyang, W., Wang, X.: Joint deep learning for pedestrian detection. In: *Proceedings of the IEEE International Conference on Computer Vision*. (2013) 2056–2063
17. Zheng, W.S., Gong, S., Xiang, T.: Associating groups of people. In: *BMVC*. Volume 2. (2009) 6
18. Li, W., Wang, X.: Locally aligned feature transforms across views. In: CVPR. (2013) 3594–3601
19. Girshick, R.: Fast R-CNN. In: *Proceedings of the IEEE International Conference on Computer Vision*. (2015) 1440–1448
20. Ouyang, W., Wang, X.: A discriminative deep model for pedestrian detection with occlusion handling. In: *Computer Vision and Pattern Recognition (CVPR), 2012 IEEE Conference on, IEEE* (2012) 3258–3265

21. Ouyang, W., Zeng, X., Wang, X.: Modeling mutual visibility relationship in pedestrian detection. In: Proceedings of the IEEE Conference on Computer Vision and Pattern Recognition. (2013) 3222–3229
22. Luo, P., Tian, Y., Wang, X., Tang, X.: Switchable deep network for pedestrian detection. In: Proceedings of the IEEE Conference on Computer Vision and Pattern Recognition. (2014) 899–906
23. Gray, D., Tao, H.: Viewpoint invariant pedestrian recognition with an ensemble of localized features. In: ECCV. Springer (2008) 262–275
24. Farenzena, M., Bazzani, L., Perina, A., Murino, V., Cristani, M.: Person re-identification by symmetry-driven accumulation of local features. In: CVPR, IEEE (2010) 2360–2367
25. Zhang, L., Xiang, T., Gong, S.: Learning a discriminative null space for person re-identification. arXiv preprint arXiv:1603.02139 (2016)
26. Kostinger, M., Hirzer, M., Wohlhart, P., Roth, P.M., Bischof, H.: Large scale metric learning from equivalence constraints. In: CVPR. (2012) 2288–2295
27. Ahmed, E., Jones, M., Marks, T.K.: An improved deep learning architecture for person re-identification. In: CVPR. (2015)
28. Ding, S., Lin, L., Wang, G., Chao, H.: Deep feature learning with relative distance comparison for person re-identification. Pattern Recognition (2015)
29. Yi, D., Lei, Z., Liao, S., Li, S.Z.: Deep metric learning for person re-identification. In: Pattern Recognition (ICPR), 2014 22nd International Conference on, IEEE (2014) 34–39
30. Zhang, N., Paluri, M., Taigman, Y., Fergus, R., Bourdev, L.: Beyond frontal faces: Improving person recognition using multiple cues. In: Computer Vision and Pattern Recognition (CVPR), 2015 IEEE Conference on, IEEE (2015) 4804–4813
31. Bourdev, L., Malik, J.: Poselets: Body part detectors trained using 3d human pose annotations. In: Computer Vision, 2009 IEEE 12th International Conference on, IEEE (2009) 1365–1372
32. Xu, Y., Ma, B., Huang, R., Lin, L.: Person search in a scene by jointly modeling people commonness and person uniqueness. In: Proceedings of the ACM International Conference on Multimedia, ACM (2014) 937–940
33. Xu, Y., Lin, L., Zheng, W.S., Liu, X.: Human re-identification by matching compositional template with cluster sampling. In: Proceedings of the IEEE International Conference on Computer Vision. (2013) 3152–3159
34. Berclaz, J., Fleuret, F., Türetken, E., Fua, P.: Multiple object tracking using k-shortest paths optimization. Pattern Analysis and Machine Intelligence, IEEE Transactions on **33**(9) (2011) 1806–1819
35. Das, A., Chakraborty, A., Roy-Chowdhury, A.K.: Consistent re-identification in a camera network. In: ECCV. Springer (2014) 330–345
36. Liao, S., Mo, Z., Hu, Y., Li, S.Z.: Open-set person re-identification. arXiv preprint arXiv:1408.0872 (2014)
37. Geiger, A., Lenz, P., Urtasun, R.: Are we ready for autonomous driving? the kitti vision benchmark suite. In: Computer Vision and Pattern Recognition (CVPR), 2012 IEEE Conference on, IEEE (2012) 3354–3361
38. Tian, Y., Luo, P., Wang, X., Tang, X.: Deep learning strong parts for pedestrian detection. In: Proceedings of the IEEE International Conference on Computer Vision. (2015) 1904–1912
39. Cai, Z., Saberian, M., Vasconcelos, N.: Learning complexity-aware cascades for deep pedestrian detection. In: Proceedings of the IEEE International Conference on Computer Vision. (2015) 3361–3369

40. Van de Sande, K.E., Uijlings, J.R., Gevers, T., Smeulders, A.W.: Segmentation as selective search for object recognition. In: *Computer Vision (ICCV), 2011 IEEE International Conference on*, IEEE (2011) 1879–1886
41. Wang, T., Gong, S., Zhu, X., Wang, S.: Person re-identification by video ranking. In: *Computer Vision–ECCV 2014*. Springer (2014) 688–703
42. Dollár, P., Appel, R., Belongie, S., Perona, P.: Fast feature pyramids for object detection. *Pattern Analysis and Machine Intelligence, IEEE Transactions on* **36**(8) (2014) 1532–1545
43. Nam, W., Dollár, P., Han, J.H.: Local decorrelation for improved pedestrian detection. In: *Advances in Neural Information Processing Systems*. (2014) 424–432
44. Yang, B., Yan, J., Lei, Z., Li, S.Z.: Convolutional channel features. In: *Proceedings of the IEEE International Conference on Computer Vision*. (2015) 82–90
45. Zheng, W.S., Li, X., Xiang, T., Liao, S., Lai, J., Gong, S.: Partial person re-identification. In: *Proceedings of the IEEE International Conference on Computer Vision*. (2015) 4678–4686